

Studies of 2-Azaazulenium Derivatives: The Natures of Electron Transitions in the 2-Azaazulenium Cation and in Monomethine Cyanine Dyes Bearing 2-Azaazulenium Moieties as Terminal Groups

Julia Bricks,^{*[a]} Aleksey Ryabitskii,^[a,b] and Alexei Kachkovskii^[a]

Keywords: Cyanines / Azaazulenes / Quantum chemistry / Absorption / Electron transfer

A series of novel monomethine cyanine dyes derived from 2-azaazulene have been synthesized. Combined spectral and quantum-chemical investigations of their molecular geometries and of their electronic structures and the natures of their lowest electron transitions have been performed. The analysis results obtained by ab initio and semiempirical methods, together with experimental data obtained from absorption and ¹³C NMR spectra, have shown that there is practically no difference between the charge distributions over the π -electron systems in the ground state in a reference 2-azaazulenium salt and in monomethine cyanines bearing 2-aza-

azulene as a terminal group, because these are not dependent on the relative locations of molecular orbitals. However, the spectral properties of – and correspondingly the natures of electron transitions in – the chromophores of the salt and of the monomethine cyanine are drastically different, due to the different mechanisms of frontier molecular orbital generation. Similar differences in properties in ground and excited states are observed for unsymmetrical monomethine cyanines.

(© Wiley-VCH Verlag GmbH & Co. KGaA, 69451 Weinheim, Germany, 2009)

Introduction

The well-known cyanine dyes have been studied for more than a century, but intensive investigations continue because their applications are permanently extending (see, for example, the latest review^[1] and references cited therein). Thanks to their strong and selective absorptions across broad spectral regions, this class of linear conjugated molecules has proved to be attractive for applications as fluorescent probes in chemistry and biology, as active and passive laser media, as photosensitizers, for optical data storage and as electroluminescence materials.^[1–5] Structural modification of these dyes, allowing shifts of their absorption bands to the near infrared (IR) region, can expand the existing areas of applications and can find new ones such as highly efficient nonlinear optical materials for all-optical signal processing.^[6] In spite of the rapidly developing available information on near-IR absorbing dyes, their thermal and photochemical stabilities and their solubilities are the main issues limiting their practical applications. There are two general synthetic methods by which to decrease the energy gap between the ground and excited states: 1) lengthening of the polymethine chain (PC), although this usually

results in a decrease in the photochemical stability,^[7,8] and 2) introduction of terminal groups with their own extended π -electron systems, hence shifting the absorption to the near-IR region through an increase in the contribution from the terminal groups to the total length of conjugation.^[9] It was shown earlier that 2-azaazulene (cyclohepta[c]pyrrole) or pseudoazulenes as terminal groups were prospective heterocycles for this purpose;^[10–12] they provide intense long-wavelength absorption in the corresponding cyanine dyes despite comparatively short PCs. In this paper we present the results of a complex spectral and quantum-chemical investigation of a reference nitrogen-substituted azulenum (cyclohepta[c]pyrrolum or azaazulenium) salt and series of symmetrical and unsymmetrical cyanines containing this heterocycle as a terminal group. The main goal was to understand the origin of the decreasing energy gap and the drastic increases in the intensities of the first electron transitions upon going from the deeply coloured azaazulenium salt **1** to the cyanine with the shortest PC (monomethine **3**), as well as to establish the dependence of the electron structures on asymmetry of the chemical constitutions of the dyes.

[a] Institute of Organic Chemistry, National Academy of Sciences of Ukraine,

5 Murmanska str., Kiev 02660, Ukraine

Fax: +38-0445732643

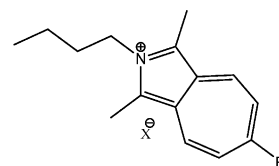
E-mail: jbricks@ioch.kiev.ua

[b] Spoluka Chemical Company,

5 Murmanska str., Kiev 02660, Ukraine

Fax: +38-0445741417

www.lifechemicals.com

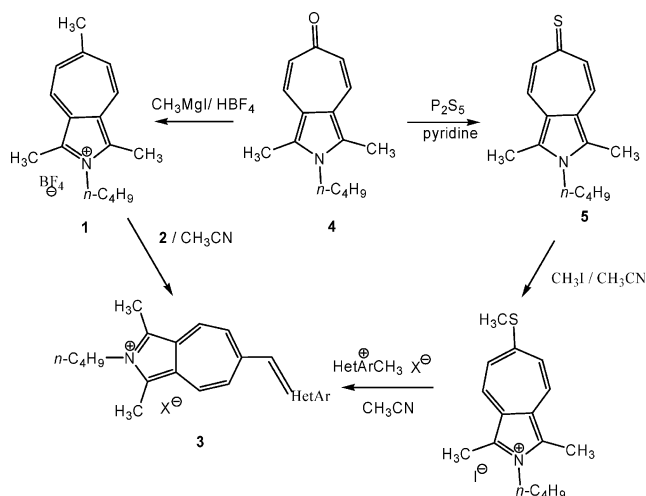


R = CH₃ (**1**), SCH₃ (**2**), CH=HetAr (**3**)

Results and Discussion

Synthesis of Azaazulene Derivatives

The general synthetic approach to the cyclohepta[*c*]pyrrolium system is presented in Scheme 1. The key compound 2-butyl-1,3-dimethylcyclohepta[*c*]pyrrol-6(2*H*)-one (**4**) and the corresponding salt **1** were synthesized accordingly,^[10] from the starting 1-butyl-2,5-dimethyl-1*H*-pyrrole-3,4-dicarbaldehyde. The preparation of 2-butyl-1,3-dimethylcyclohepta[*c*]pyrrole-6(2*H*)-thione (**5**) and the corresponding methylthio-substituted derivative **2** has been described in the literature.^[13]



Scheme 1. Synthesis of 2-azaazulenium derivatives.

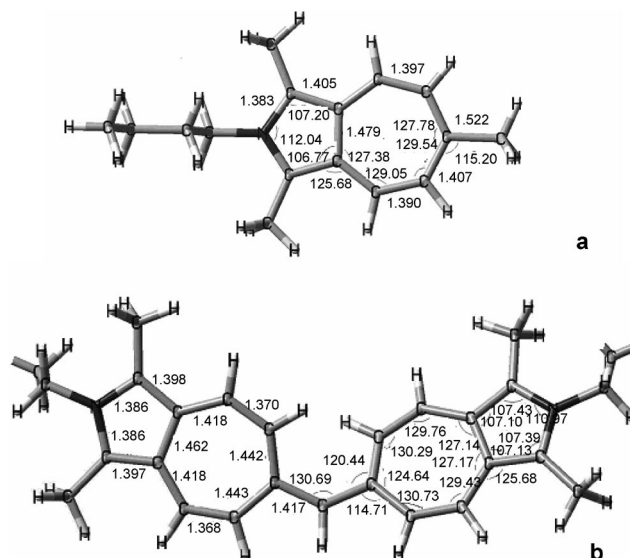
Table 1. Spectral properties of monomethine cyanine dyes **3**.

Dye	HetAr (X [−])	Absorption spectra, CH ₃ CN	
		λ_{max} [nm] ($\epsilon \cdot 10^{-4}$, M ^{−1} cm ^{−1})	$\Delta\nu_{1/2}$ [cm ^{−1}]
3a		708 (11.03), 316 (2.78), 244 (3.71)	1374.2
3b		624 (5.44), 376 (1.17), 330 (1.38), 290 (1.75), 246 (2.68)	2954.9
3c		558 (5.69), 326 (1.17), 274 (1.78)	3194.2
3d		698 (4.43), 303 (1.85), 244 (1.78)	2185.0
3e		588 (3.85), 292 (2.39)	3446.9
3f		532 (5.35), 496 (5.56), 310 (1.65)	3874.2

The series of symmetrical and asymmetrical monomethine cyanine dyes **3** were synthesized by conventional cyanine chemistry synthetic approaches. The spectral properties of the new dyes are presented in Table 1.

Optimized Molecular Geometry in the Ground State

The azaazulenium (AA) cation could be regarded as a nitrogenous analogue of the non-alternant π -electron cyclic hydrocarbon azulene, which is responsible for some features of the equilibrium molecular geometry and the distribution of the electron density over atoms within the two rings. The calculated (by the DFT method) lengths of carbon–carbon and carbon–nitrogen bonds, as well as valence angles for the AA cation **1** and symmetrical monomethincyanine **3a**, are presented in Figure 1.

Figure 1. DFT-optimized structures and selected geometrical parameters [Å, °] for: a) AA salt **1**, and b) monomethine dye **3a**.

As can be seen in Figure 1, the π electron system in the AA cation is planar. C–C bond lengths are practically aligned and are equal to the bond length in a cyanine chromophore,^[13] about 1.40 Å, with the exception of the bond common to both the seven- and the five-membered rings, which is lengthened to 1.479 Å. The values of the valence angles in the salt **1** are somewhat increased in comparison with an ideal linear conjugated system with sp^3 -hybridized carbon atoms, at about 130°. In contrast with the AA cation **1**, the monomethine cyanine cations **3** are nonplanar, due to considerable steric hindrance between the heterocyclic terminal groups. In accordance with quantum-chemical calculations (B3LYP/3–21G**), the terminal groups in symmetrical dye **3a** in the ground state are twisted by about 36° (Figure 1, b). Such a disruption of planarity is the result of the close spatial arrangement of the protons in positions 7 and 7', along with the rotation of the AA cycles about the C6–C11 bond.

Such nonplanar conformations are not observed for all structures investigated by us, however, and we managed to investigate these peculiarities of the conformational behaviour by NMR spectroscopy. On the other hand, this strong distortion of the planar constitution in dye molecules **3** resulted in disruption of the equalization of bond lengths in the AA cyclic fragments. Calculations thus predict the emergence of alternation of the CC bonds along the cyanine chromophore, including both the open chain and the terminal groups from one nitrogen atom to the other (the so-called Kuhn's chain).^[19]

Charge Distribution and ¹³C NMR Signals

The non-alternant nature of the chemical constitution causes the alternation of the charges at neighbouring atoms in the AA π system, similarly to the charge distribution along chromophores of the cationic polymethine dyes. As

can be seen in Figure 2 (a) and Table 2, in which we present the calculated charges (q) at carbon atoms, the alternation of electron density in the seven-membered cycle is much more pronounced than in the azole ring.

In the last case the charges at the neighbouring carbon atoms are rather equalized, apparently because of the influence of the more electron-withdrawing nitrogen atom. On going to the monomethine cyanine **3a**, the nature of the charge distribution does not change in principle: substantial alternation of the electron density at the neighbouring carbon atoms over all the cyanine chromophore (Kuhn's chain) is observed, as it is typical for polymethine dyes.^[14–19]

For the experimental confirmation of the character of charge distribution in the chromophore one can use NMR chemical shifts, such as $\delta_{\mu}(^{13}\text{C})$, which are correlated with quantum-chemically accessible electron density values (q_{μ}) in atoms.^[15] The obtained experimentally measured ¹³C NMR chemical shifts and the calculated charges on the carbon atoms are collected in Table 2.

In Figure 2 (b) we present chemical shifts [$\delta_{\mu}(^{13}\text{C})$] of the AA cation **1** and the symmetrical monomethine cyanine **3a**. There is an essential alternation of the magnitudes of chemical shifts for neighbouring carbon atoms both in the heterocycle **1** and in the dye **3a**, which is in good agreement with the charge density distributions for both these cations (Figure 2, a). As mentioned above, some of the investigated dyes were predicted to exist as nonplanar molecules, due to the hindered rotation about the CC bond connecting the methine (chain) carbon atom and the C6 atom in the heterocycle. According to DFT calculations for the ground state, only compound **3f** should have a planar constitution.

Experimentally, the fact of such a rotation was confirmed by ¹H and ¹³C NMR spectroscopy, in which we observed non-equivalent signals for proton and carbon atoms at positions 5/7 and 4/8 (see Table 2), so we can assume that the hindered rotation takes place just around the C6–C11 bond. Visible broadening of proton signals H5/H7 and H4/H8, associated with slow intramolecular rotation relative to the

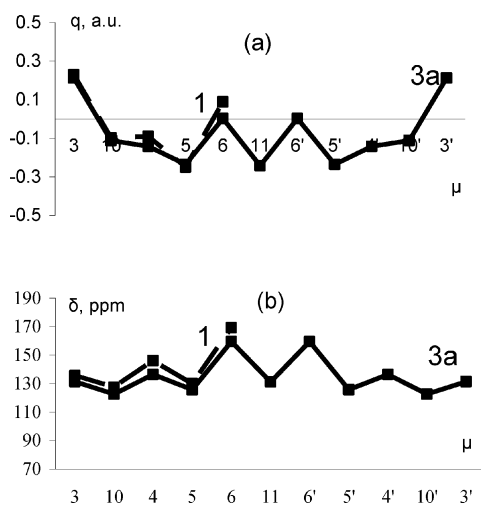
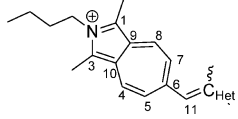


Figure 2. a) Calculated charge distribution (B3LYP/3-21G** NBO). b) ¹³C NMR shifts (CDCl₃) for compounds **1** (dashed line) and **3a** (solid line).

Table 2. The experimentally measured chemical shifts of the ¹³C NMR signals and the corresponding calculated charges for the salt **1** and the monomethines **3a–f**.



C atom	1 ^[a]	3a ^[a]	3b ^[a]	δ , ppm; q, a.u. (B3LYP/3-21G**; NBO)			
				3c ^[b]	3d ^[a]	3e ^[b]	3f ^[a]
1	135.64/0.233	131.40/0.213	131.89/0.218	–/0.223	132.29/0.217	129.76/0.215	130.83/0.219
3	135.64/0.233	131.40/0.213	131.89/0.217	–/0.217	132.29/0.219	129.76/0.215	130.07/0.217
9	127.39/–0.097	122.62/–0.113	122.96/–0.114	–/–0.115	123.45/–0.113	118.83/–0.116	121.41/–0.113
10	127.39/–0.097	122.62/–0.111	122.96/–0.111	–/–0.111	123.45/–0.112	118.83/–0.113	121.38/–0.111
4	146.14/–0.090	136.38/–0.144	139.10/–0.139	133.70/–0.138	138.16/–0.135	129.20/–0.143	135.27/–0.133
8	146.14/–0.090	136.38/–0.140	139.10/–0.133	136.80/–0.123	138.16/–0.135	131.20/–0.138	136.71/–0.126
5	130.00/–0.250	125.71/–0.235	126.25/–0.238	127.20/–0.241	125.89/–0.242	127.00/–0.239	127.45/–0.245
7	130.00/–0.250	125.71/–0.258	126.25/–0.264	117.50/–0.273	125.89/–0.265	117.80/–0.265	111.41/–0.260
6	169.17/0.089	159.61/0.003	159.40/0.014	157.30/0.022	156.17/0.015	151.87/0.009	160.55/0.030
11	29.85/–0.709	131.18/–0.243	122.38/–0.261	105.77/–0.350	111.78/–0.302	116.18/–0.271	92.80/–0.388
C _{Het}	–	159.61/0.003	149.61/–0.001	161.82/–0.395	161.80/0.262	152.24/0.024	159.94/0.571

[a] Recorded in CDCl₃, [b] Recorded in [D₆]DMSO.

NMR timescale at the experiment temperature (293 K), was also observed. The same broadening of the corresponding signals was also observed in the ^{13}C NMR spectra: in the case of compound **3c**, for example, it was possible to achieve the full assignment of ^{13}C chemical shifts for atoms C4, C5, C7 and C8 by use of heteronuclear correlation C–H spectra from the positions of correlation peaks, but it was not possible to identify the chemical shifts for the quaternary atoms C1, C3, C9 and C10, due to their strong broadening.

The differences in chemical shifts were particularly apparent in the case of the monomethine **3f**, containing a benzoxazole moiety as the second terminal group, which exists in the most planar conformation predicted by calculations. For this dye we observed non-equivalence of the signals of the methyl group carbon atoms ($\text{CH}_3\text{--C1}$ and $\text{CH}_3\text{--C3}$), the magnetically non-equivalent moieties most remote from the methine atom of the molecule.

It is thus possible to have confidence that the planar conformation is the most energetically favourable for molecules of such a type, and that it will always be achieved if this is allowed by the spatial structure. It is permissible to assume that the energy barriers of rotation are higher for monomethine cyanines with planar conformations, as a consequence of the maximal conjugation of the electronic system.

It has been proposed^[14] that the alternation amplitude (Δq_μ) calculated by Equation (1) as the difference in electron densities at neighbouring atoms (q_μ and $q_{\mu+1}$, correspondingly) is a more suitable parameter with which to analyse the influence of the molecular topology and asymmetry on the shape and location of the charge wave.

$$\Delta q_\mu = (-1)^\mu (q_\mu - q_{\mu+1}) \quad (1)$$

For convenience, the solitonic waves can sometimes be described by the modulus of the parameter $|\Delta q_\mu|$ (scalars). It has been proposed^[14] that the value $|\Delta q_\mu|$ may be considered a parameter of the “ionicity” of the bond between two neighbouring atoms μ and $\mu+1$. Taking the relationship between the calculated electron densities and NMR signals into consideration,^[15] we can also write a similar function for the alternation of the experimentally observed characteristics $\delta_\mu(^{13}\text{C})$ [Equation (2)].

$$\Delta \delta_\mu = (-1)^\mu (\delta_\mu - \delta_{\mu+1}) \quad (2)$$

Figure 3 shows graphic charts depicting amplitudes of charge alternation (Figure 3, a) and NMR signals $\delta_\mu(^{13}\text{C})$ (Figure 3, b) for compounds **1** and **3a–f**. Apparently, the degree of alternation reaches its maximum at position C-11. The AA heterocycle as a terminal group in the symmetrical monomethine cyanine **3a** and the unsymmetrical dyes **3b–f** could thus be considered a direct (branched) extension of the polymethine chromophore of the opened chain that is equal to four bonds for each end group.

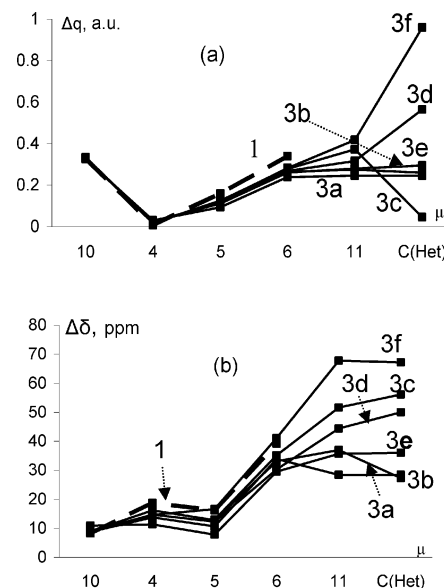


Figure 3. (a) Alternation of calculated charge distribution (B3LYP/3–21G** NBO). (b) Experimentally observed ^{13}C NMR shifts (CDCl_3) for compounds **1** and **3a–f**.

Generation of the Frontier and Nearest Molecular Orbitals

In spite of the fact that the electronic structures of the monomethine cyanine chromophores **3** and that of the starting salt **1** in the ground state are similar (typical cyanine-like structures), their absorption spectra are fundamentally different. Before starting the analysis of the natures of the electron transitions related to the spectral bands in order to understand the reasons for such a difference, let us examine the generation of molecular orbitals in the conjugated systems of cations **1** and **3a**.

It was shown previously^[20] that terminal groups with their own highly localised orbitals can make determining contributions to the highly occupied MOs of cyanine dyes with comparatively short PCs. On the other hand, going from neutral molecules to ions of conjugated systems leads to fundamental shifts of the bands of both vacant and occupied levels.^[21] In the case of anions, the values of the energies of the bands of both vacant and occupied levels increase, whereas in the case of cations these values decrease. In cases of cationic polymethine dyes containing heterocyclic terminal groups with donating nitrogen, donating properties are provided by the lone electron pair of the nitrogen atom conjugated with polymethine chromophore. If it is taken into account that the positive charge should be localized in a chromophore consisting of the external chain and the carbon atoms of AA terminal groups it is possible to present, for example, the symmetrical dye **3a** as the system $\text{D--}\pi(+)\text{--D}$ or D--A--D , where the acceptor A is a polymethine chain.

Because of the additional electrons (in relation to the corresponding unsubstituted molecule) the conjugated system is turned into a charge-excessive one, just keeping the

same total charge. As a result, the energy gaps in conjugated systems with donor terminal groups are shifted to higher-energy regions than in the case of unsubstituted polymethine cations.^[21] Consequently, as has been shown for known cationic cyanines containing indolenine, benzo-thiazole, pyridine etc. residues as terminal groups, two highest occupied MOs (HOMOs) are formed first of all, due to donor terminal groups. It has therefore been suggested that these orbitals can be considered as donor orbitals, especially in cases of dyes with short chains. To the first approximation they could be represented by symmetrical and unsymmetrical linear combinations of the HOMOs of each two terminal groups $\phi(D_1)$ and $\phi(D_2)$, as in Equations (3) and (4).

$$\phi_1 = (2)^{-1/2} \{ \phi(D_1) + \phi(D_2) \} \quad (3)$$

$$\phi_2 = (2)^{-1/2} \{ \phi(D_1) - \phi(D_2) \} \quad (4)$$

That is, the two corresponding levels could be interpreted as two split donor levels, in which the PC is considered to be a common external conjugated substituent for each donor D.

Figure 4 shows the schemes of formation of frontier and closed MOs participating in lowest electron transitions for reference salt **1** and monomethine cyanine cations **3**. The analysis has shown that the mechanism of HOMO formation in the case of AA-based dyes is differed from the scheme described above for indocyanines and their hetero analogues. The π -system of salt **1** is symmetric with a C_{2v} symmetry group; antisymmetric MOs therefore have nodes at the nitrogen atom and the carbon atom at position 5 (Figure 4, a). Upon formation of the general conjugated π -electron system of dye **3a**, the heterocyclic terminal groups also remain (to the first approximation) symmetric (accurate within Coulomb's interaction) with preservation of MO nodal properties.

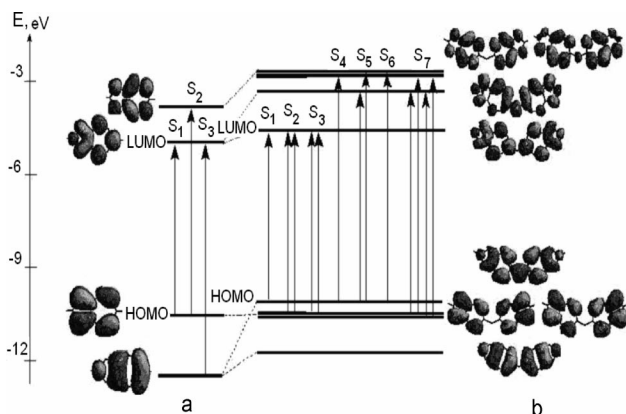


Figure 4. Molecular orbitals and electron transitions in: a) AA salt **1**, and b) monomethine cyanine **3a**.

The HOMO of the salt **1**, and consequently of the corresponding orbital of the terminal group (Figure 4, a), thus each have the node at the carbon atom C-6 connected in

dye **3** with the chain, so this orbital does not conjugate with the polymethine chromophore, and remains a local MO. Other antisymmetric orbitals – (LUMO+1), for example – remain local too. From Figure 4 it is obvious that the non-zero coefficient at the place of connection of the terminal heterocycle with a PC has HOMO–1; just its interaction with the same orbital of the terminal group (and also with a PC) leads to a splitting of the corresponding levels and to formation, as a first approximation, of two new MOs, according to Equations (3) and (4) symmetric and antisymmetric. As can be seen from Figure 4 (b), the interaction energy is considerable, so that one of the split orbitals (the symmetric one) appears to be the HOMO whereas the energy of the antisymmetric orbital is much less than that of the HOMO of the initial salt. Because the π system of the cationic dye **3a** is electron-excessive, its occupied levels are shifted upwards relative to the levels of the electron-balanced π -system of the salt **1**.

At the same time, from the antisymmetric HOMOs of both AA end-groups, two degenerate orbitals of opposite symmetry are formed: HOMO–1 and HOMO–2, with energies practically the same as the HOMO energy of the initial salt **1** (see parts a and b of Figure 4). The next orbital of lower energy, HOMO–3, proves to be the antisymmetrically split MO. Two lower vacant orbitals, LUMO and LUMO+1, are split; the corresponding levels are shifted upwards. The interaction of the rest of the MOs of both terminal groups and the single orbital formed by the carbon atom at C11 of the PC of dye **3a** could be analysed analogously.

However, the essential change in the nature of the occupied MO upon going from the salt **1** to the monomethine cyanine does not influence the character of charge distribution in the ground state, because of the fact that the molecular orbitals in the closed electron shell are invariant with respect to any orthogonal transformation,^[22] because by definition of electronic density in each atom, contributions of every MO in all shells are summarized. Therefore, the specific cyanine-like type of charge distribution, with the considerable alternation of the electron density in the neighbouring carbon atoms within the chromophore, is similar both for the initial AA salt **1** and for the dyes **3**, despite drastic differences in the natures of their HOMOs.

The distinction in the formation of the frontier and the next-nearest MOs in the cyanine dyes that are derivatives of, for example, indolenine or its heteroanalogues, and in the cyanines that are derivatives of azaazulene should affect, first of all, the natures of the electron transitions and the redistribution of electron density upon excitation.

Absorption Spectra and Electron Transitions

Figure 5 demonstrates UV/Vis absorption spectra of the AA salt **1** and of the symmetrical monomethine cyanine **3a** in acetonitrile. One can see that these spectra differ crucially first of all in their intensities and shapes, in spite of the similar characters of the charge distributions in the π sys-

tems of the two cations. In the absorption spectra of salt **1** a weak-intensity broad band with a maximum at 634 nm is observed, typical of electron transitions with intramolecular charge transfer (CT) transition.^[18,23]

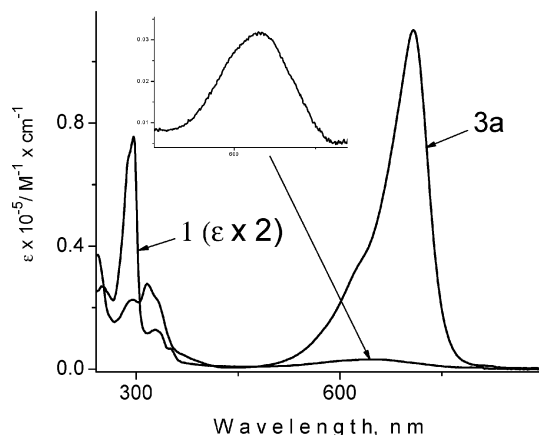


Figure 5. Absorption spectra of AA salt **1** (solid line) and monomethine **3a** (dashed line) in acetonitrile.

At the same time, there is a narrow and comparatively intense band with a maximum at 298 nm in a short-wavelength region, similar to long-wavelength absorption bands of polymethine cyanines (cyanine-like spectral band). Vice versa, a long-wavelength band of monomethine cyanine **3a** is the typical cyanine-like band. Its absorption band half-width ($\Delta\nu_{1/2} = 1374 \text{ cm}^{-1}$) is close to $\Delta\nu_{1/2}$ values for symmetrical and unsymmetrical cyanine dyes ($\Delta\nu_{1/2} = 900\text{--}1100 \text{ cm}^{-1}$)^[24,25] but at the same time, it is drastically different from this parameter for polyene-like cyanine bases ($\Delta\nu_{1/2} = 3000\text{--}4000 \text{ cm}^{-1}$).^[25] In the short-wavelength region, absorption bands of comparable intensity with maxima at 316 nm and 244 nm are observed; these are close to the intensive band of the salt **1** with $\lambda_{\text{max}} = 298 \text{ nm}$.

Quantum-chemical calculations of characteristics of the excited states for the salt **1** and the symmetrical cyanine dye **3a** were performed for interpretation of the observed absorption bands and identification of the corresponding electron transitions; the results are collected in Table 3. It should be noted preliminarily that the energies of transition (both singlet and triplet) could be estimated not only by the distance between the corresponding levels, but also by the electron interaction between them according to Equations (5) and (6).^[22]

$$\Delta E(S_0 \rightarrow S_p) = \varepsilon_j - \varepsilon_i + 2K_{ij} - J_{ij} \quad (5)$$

$$\Delta E(S_0 \rightarrow T_p) = \varepsilon_j - \varepsilon_i - J_{ij} \quad (6)$$

where ε_j and ε_i are the energies of the vacant and the occupied MO involved in the transition, respectively, and J_{ij} and K_{ij} are Coulomb and resonance integrals.

It was found that there was a serious problem in the correlation between the calculated and experimentally observed energies both for the first and for higher electron transitions. In practice, it is the magnitudes of the parameter OWF (overlap weight factor) in the other semiempirical

Table 3. Calculated spectral characteristics of AA salt **1** and monomethine cyanine **3a** (ZINDO/S).

Compd.	Transition	λ [nm]	f	Main configuration, $T_{p,i \rightarrow j}$
1	$S_0 \rightarrow S_1$	632	0.104	$ S_1\rangle = 0.99 H \rightarrow L\rangle$
	$S_0 \rightarrow S_2$	353	0.124	$ S_2\rangle = 0.88 H \rightarrow L+1\rangle$
	$S_0 \rightarrow S_3$	264	1.940	$ S_3\rangle = 0.88 H-1 \rightarrow L\rangle$
3a	$S_0 \rightarrow S_1$	708	1.186	$ S_1\rangle = 0.98 H \rightarrow L\rangle$
	$S_0 \rightarrow S_2$	669	0.076	$ S_2\rangle = 0.73 H-1 \rightarrow L\rangle$ $-0.57 H-2 \rightarrow L\rangle$
	$S_0 \rightarrow S_3$	655	0.084	$ S_3\rangle = 0.56 H-1 \rightarrow L\rangle$ $+0.74 H-2 \rightarrow L\rangle$
	$S_0 \rightarrow S_4$	422	0.007	$ S_4\rangle = 0.95 H \rightarrow L+2\rangle$
	$S_0 \rightarrow S_5$	417	0.004	$ S_5\rangle = 0.48 H \rightarrow L+1\rangle$ $+0.62 H \rightarrow L+3\rangle$
	$S_0 \rightarrow S_6$	402	0.007	$ S_6\rangle = 0.73 H \rightarrow L+3\rangle$
	$S_0 \rightarrow S_7$	381	0.927	$ S_7\rangle = 0.54 H-1 \rightarrow L+1\rangle$ $-0.48 H-1 \rightarrow L+2\rangle$ $-0.48 H-2 \rightarrow L+1\rangle$ $-0.45 H-2 \rightarrow L+2\rangle$

method ZINDO/S, which are connected indirectly with the overestimation of the electron–electron repulsion ($\gamma_{\mu\nu}$) used in the integrals J_{ij} and K_{ij} . This is calculated by the Mataga–Nishimoto formulas: $\gamma_{\mu\nu} = a/(1+R_{\mu\nu})$, where a is a constant and $R_{\mu\nu}$ is the distance between the μ th and the ν th atoms, for atoms a great distance apart from each other. The same problem of the integrals $\gamma_{\mu\nu}$ has been found to exist even in the simplest PPP approximation taking electron–electron interaction correctly into consideration. Tyutyulkov proposed the modifying formula $\gamma_{\mu\nu} = a/(1+t R_{\mu\nu})$, where $t = 10/3$;^[26] the agreement between the calculated and experimentally measured wavelengths of the first electron transition for the vinyllogous series of the polymethine dyes was thus fundamentally improved.^[27] In this paper we have used the same parameter OWF for the first and higher electron transitions, optimistically postulating that the divergence between the theoretical and experimentally determined transition energies should not be so considerable as to prevent correct establishment of the order of the transitions of the different types (cyanine-like transition or transition with the charge transfer – CT). The central and most important part of our work was to establish the natures of the first and higher transitions in the AA cation **1** and cationic cyanines **3** and hence to explain correctly the main reason for the fundamental difference between their spectra.

Firstly, let us discuss the natures of electron transitions in the AA cation. As is evident from Table 3, the first transition – $S_0 \rightarrow S_1$ – has the configuration with single-occupied frontier MO: $|S_1\rangle = 0.99 |H \rightarrow L\rangle$. Because of the opposite symmetries of participating orbitals, the first transition is antisymmetrical: $1A_1 \rightarrow 1B_1$ (symmetry group C_{2v} ; the ground state with closed electron shell is totally symmetrical, $1A_1$) and is polarized along the PC.

Diagrams of charge redistribution atoms upon excitation have proved to be a very useful tool for analysis of the natures of charge transitions.^[28,29] The changes in electron densities upon transition to the excited state in cation **1** could be estimated by Equations (7) and (8).

$$\delta q_{\mu} = (q_{\mu}^* - q_{\mu}^{\circ}) \quad (7)$$

$$\delta p_{\nu} = (p_{\nu}^* - p_{\nu}^{\circ}) \quad (8)$$

where the parameters q_{μ}^* and p_{ν}^* correspond to the excited state, and q_{μ}° and p_{ν}° correspond to the ground state.

Figure 6 presents diagrams of redistribution of electronic densities in cation **1**. Apparently, the first transition is accompanied, mainly, by electron density transfer from the five-membered azole ring (electron-excessive in the ground state) to the electron-deficient seven-membered ring; that is, it is a typical CT transition. This enables us to explain the specific broad and low intensive absorption band as well as the comparatively deep colour of the AA cation, like the deep colour of azulene itself: $\lambda_{\max} = 575 \text{ nm}$.^[30]

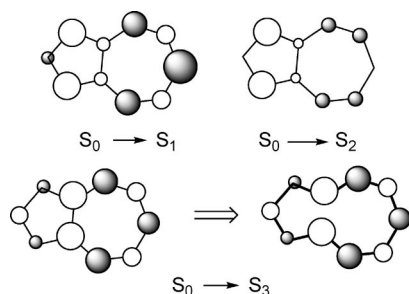


Figure 6. Electron density redistribution upon electron transition for the AA salt **1**: empty circle – electron density decreases, full circle – electron density increases.

Calculations indicate that the next two transitions, as it is evident from Table 3, should be also practically “pure” (i.e., each of them is described mainly by one configuration). From Figure 4 it is clear that orbitals participating in these transitions are of the same symmetry, so transitions $S_0 \rightarrow S_2$ and $S_0 \rightarrow S_3$ are symmetric, correspondingly: $1A_1 \rightarrow 2A_1$, $1A_1 \rightarrow 3A_1$, and hence they are polarized perpendicularly to a long axis of a molecule. The energies of these transitions are considerably higher than the energy of the first transition. The transition $S_0 \rightarrow S_2$ is accompanied by transfer of electron density from the azole ring to the seven-membered one (see Figure 6), similarly to the first transition, but the value of this charge transfer is much less. The calculated oscillator strength (f_2) is very close to the value f_1 , so the transition $S_0 \rightarrow S_2$ could correspond to the experimentally observed low-intensity band $\lambda_{\max} = 295 \text{ nm}$, although according to the calculations (with the same OWF parameter) the wavelength value of this transition should be longer: $\lambda_2^{\text{calc}} = 353 \text{ nm}$.

The calculations predict a large oscillator strength value for the $S_0 \rightarrow S_3$ transition; in the absorption spectra the narrow and comparatively intense band with $\lambda_{\max} = 298 \text{ nm}$ could be attributable to it (taking into account the tendency of calculations to overestimate the results). The charge-redistribution diagram (Figure 6) demonstrates the third transition to be accompanied by the transfer of electron density to the neighbouring atoms, typical of the first, cyanine-like, transitions in polymethine dyes.^[28,29] The picture would look more demonstrative if the bond common to both five-

and seven-membered rings were removed virtually. The transition $S_0 \rightarrow S_3$ could be interpreted as cyanine-like. If the *all-cis* conformation of the corresponding chromophore is taken into account, the polarization of the transition $S_0 \rightarrow S_3$ is similar to the polarization in the typical cyanines: along the chromophore.

Thus, both transitions – $S_0 \rightarrow S_1$ and $S_0 \rightarrow S_2$ from HOMO to LUMO and to LUMO–1 – are correspondingly CT transitions, whereas the transition involving HOMO–1 ($S_0 \rightarrow S_3$) is similar to the cyanine-like transition in the cationic and anionic polymethine dyes. The HOMO–1 could then be regarded as a cyanine-generating orbital.

As described above, just this orbital takes part in the generation of the HOMO in cyanine dye **3a** (Figure 4; i.e., in a monomethine cyanine the high occupied level is cyanine-like). Consequently, the first transition – $S_0 \rightarrow S_1$ – involving the frontier levels is the cyanine-like electron transition, and corresponds to the observed high-intensity and narrow long-wavelength spectral band, in contrast to the CT transition nature of the first transition in the salt **1b**.

Substantial splitting of donor levels (HOMO and HOMO–3), as well as equalization of bond lengths usual for cationic dyes and low disposition of the LUMO, is responsible not only for the considerable decrease in gap energy but also for the increases in integrals K_{ij} and J_{ij} in Equation (5). As a result, a bathochromic shift of the absorption band, relative to the absorption maximum of the initial salt **1**, is observed (Figure 5).

The cyanine-like nature of the first electron transition is confirmed by the corresponding charge-redistribution diagram (Figure 7). One can see that the excitation is accompanied by transfer of electron density to the neighbouring atoms, typical of the first transitions – $S_0 \rightarrow S_1$ – in polymethine dyes.

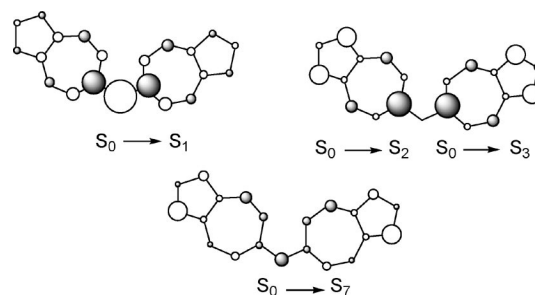


Figure 7. Redistribuition of the electron density upon excitation in the case of dye **3a**.

Due to the opposite symmetries of the HOMO (b_2) and LUMO (a_2) participating in the transition, the first excited state is antisymmetric – $1B_1$ – so the transition $1A_1 \rightarrow 1B_1$ is polarized along the chromophore. It is hence characterized by considerable transition dipole moment and consequently by essential oscillator strength. This is in agreement with the comparatively high intensity of the long-wavelength absorption band, in contrast to the low-intensity CT transition band in salt **1**.

Quantum chemical calculations show that the next two transitions – $S_0 \rightarrow S_2$ and $S_0 \rightarrow S_3$ – correspond to mixtures of configurations with consequent participation of one of the degenerate MOs formed from the HOMO of the initial salt with the node in an atom connected with the chain (see Table 3). As can be seen from Figure 4, the antisymmetric LUMO of cyanine **3a** has its node in the C11-position. As a result, both transitions are localized at the terminal groups. The electron density redistribution diagrams demonstrate that the natures of transitions $S_0 \rightarrow S_2$ and $S_0 \rightarrow S_3$ are both practically the same as the nature of the first electron transition for the salt **1** (compare the corresponding diagrams from Figure 6 and Figure 7). One can see from Table 3 that the calculated wavelengths – $\lambda_2 = 669$ nm and $\lambda_3 = 655$ nm – are close to the magnitude $\lambda_1 = 708$ nm for the first transition; at the same time, the oscillator strengths of f_2 and f_3 are both more than one order of magnitude weaker than f_1 . We can therefore argue that in the absorption spectrum of monomethine cyanine **3a** the low-intensity bands corresponding to the transitions $S_0 \rightarrow S_2$ and $S_0 \rightarrow S_3$ should be covered by the intensive long-wavelength band generated by the first transition. As follows from the calculations (Table 2), the transitions $S_0 \rightarrow S_4$, $S_0 \rightarrow S_5$ and $S_0 \rightarrow S_6$ should also be low-intensity and could be invisible in the absorption spectrum. Only transition $S_0 \rightarrow S_7$, including local orbitals HOMO–1 and HOMO–2 as well as two LUMOs with the rather large oscillator strength $f_7 = 0.927$, could manifest itself as a comparatively intense spectral peak. We assume that the band with $\lambda_{\max} = 316$ nm corresponds to this transition. Figure 7 shows that the transition $S_0 \rightarrow S_7$ is accompanied mainly by the transfer of electron density from the five-membered azole cycles of the terminal groups to the acceptor seven-membered rings, as well as to the carbon atom at C11 (i.e., it is similar to the CT transition).

In the absorption spectra of unsymmetrical monomethine cyanine dyes we observe changes in the positions of the absorption bands, as well as in their shapes and, especially, in the widths of the spectral bands (Figure 8).

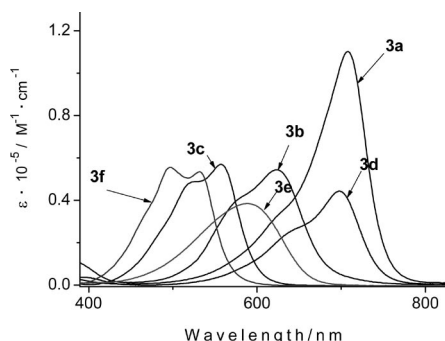


Figure 8. Absorption spectra of monomethine dyes **3** in acetonitrile.

Of course, the band positions are dependent on the effective lengths of the second terminal groups, which can be estimated experimentally by the expression^[31] $L^{\text{eff}} = (\lambda_{\max} - n \cdot V)/V$, where V is the vinylene shift in vinylogous series of

symmetric dyes with the terminal group of interest, and n is the number of vinylene groups in the PC.

For symmetrical trimethine cyanine ($n = 1$) derivatives of 2-azaazulenium, 4-pyrylium, benzothiazolium, benz[*c,d*]indolium, 4-quinolinium and benzoxazolium the corresponding values of parameters L^{eff} are 6.40, 6.07, 4.00, 6.50, 4.35, 3.48, respectively. To a first approximation, one can assume the following expression for the unsymmetrical monomethine cyanines: $\lambda_{\max} \approx (L^{\text{eff}}_1 + L^{\text{eff}}_2)/2$. Indeed (see Figure 6, Table 1), hypsochromic shifts of the absorption bands are observed for the monomethine cyanines **3b**, **3c**, **3e**, **3f** containing the second terminal groups characterized by the essentially smaller parameters of the effective length. At the same time, the absorption band almost does not shift in the spectrum of dye **3d**, so far as the magnitude L^{eff} for the benz[*c,d*]indolium residue is close to this parameter for the AA terminal group. It is known^[32] that differences in the basicities of the terminal groups are the second factor that influences the positions of absorption bands in unsymmetrical dyes. In the case of monomethine cyanines it is difficult to take this factor into account, however, because of considerable steric hindrance in the molecules that could distort the spectral influence of non-equivalence of donor properties of the terminal groups. In the same way, the difference in basicities, as well as possible steric effects, could considerably influence the bandwidths of unsymmetrical dyes.

Conclusions

Analysis of quantum chemical calculations and experimental spectroscopic data has thus shown that there is practically no difference in charge distribution over the π electron systems in the ground state in the AA salt **1** and in the monomethine cyanines **3** containing azaazulene systems as terminal groups, because the charge distributions are not dependent on the relative locations of the MOs. At the same time, the spectral properties, and correspondingly the nature of electron transitions in the chromophores, of compounds **1** and **3** are drastically different because of the different mechanisms of generation of the HOMOs. Similar differences in properties in the ground and in excited states are observed for unsymmetrical monomethine cyanines.

Experimental Section

General: UV/Vis absorption spectra were recorded on a Shimadzu UV-3100 spectrophotometer. All NMR measurements were carried out on a Varian Gemini 2000 spectrometer with ^1H and ^{13}C frequencies of 400.07 and 100.61 MHz, respectively, at 293 K. Tetramethylsilane was used as a standard for δ scale calibration. ^1H NMR spectra were recorded with spectral widths of 8000 Hz and 32000 points. ^{13}C NMR spectra were recorded with spectral widths of 30000 Hz and 128000 points. ^1H – ^1H COSY^[33] spectra were acquired in a 2048 (F2) and 512 (F1) time-domain data matrix and a 2048 (F2) \times 2048 (F1) frequency-domain matrix after zero-filling. NOESY^[34] spectra were acquired, if necessary, with parameters similar to COSY spectra. Mixing times were determined prelimi-

narily from a T_1 measurement experiment for each sample by a conventional inversion-recovery method. Heteronuclear chemical shift correlation (HETCOR)^[35] was used to determine ^1H – ^{13}C attachment with the $2048 (F_2) \times 256 (F_1)$ time-domain matrix and the $2048 (F_2) \times 1024 (F_1)$ frequency-domain matrix after zero-filling. The average value of one bond constant ($J_{\text{C,H}}$) was set to 140 Hz. HETCOR for determination of long-range correlation had very similar parameters and the average value of the multibond C–H coupling constant was set to 8 Hz.

The quantum chemical calculations were performed to study the dependence of the electronic structures and electron transitions on the molecular constitutions. The equilibrium geometries of dye molecules in the ground state were optimized by use of the GAUSSIAN98^[36] program set within the DFT approximation. A functional B3LYP^[37] was chosen, in combination with the standard 3–21G** basis sets. In cases in which structures were needed conformational analysis was carried out by scanning of the potential energy surface to search for the optimal conformation with the energy minimum. For the optimized geometry the calculation of force constants and the resulting vibrational frequencies was performed; the procedure was stopped at an energy gradient of $0.01 \text{ kcal mol}^{-1}$.

Charge distributions in atoms were calculated by the theory of Natural Bond Orbital analysis (NBO).^[38] The electron transition characteristics were calculated with the program package HyperChem. 6.0^[39] by the ZINDO/S method using, as a rule, all the π electron single excited configurations; the empirical parameter OWF (Overlap Weight Factor) was varied to achieve the best agreement between the calculated and spectral energy of the first electron transition. We could then analyse the shape of the molecular orbital as well as the nature of the lowest and higher electron transitions.

The starting materials and solvents for the synthesis and spectroscopic measurements were purchased from Aldrich.

2-Butyl-1,3,6-trimethylcyclohepta[c]pyrrolium Tetrafluoroborate (1): A solution of ketone **4** (5.0 g, 21.8 mmol) in anhydrous THF (25 mL) was added dropwise at room temperature under argon to the Grignard reagent prepared in the usual way from magnesium (2.09 g, 87 mmol) and methyl iodide (12.37 g, 87 mmol) in anhydrous reagent grade diethyl ether (95 mL). The solution was partly discoloured with the precipitation of a yellow solid. The resulting mixture was stirred at 40°C for 2 h. The solvent was then evaporated in vacuo, which was followed by addition of a mixture of acetic acid (40 mL) and HBF_4 (50%, 30 mL). The resulting blue solution was poured into water (500 mL). After 12 h the product was extracted with dichloromethane ($5 \times 50 \text{ mL}$) and dried with Na_2SO_4 . After evaporation of solvent the solid was triturated with diethyl ether, yielding the salt **1** (4.7 g, 68.3%). An analytical sample was purified by recrystallization from isopropanol; m.p. 105 – 107°C . ^1H NMR: $\delta = 8.74$ [d, $^3J(\text{H,H}) = 10.4 \text{ Hz}$, 2 H, 4-H, 8-H], 7.50 [d, $^3J(\text{H,H}) = 10.4 \text{ Hz}$, 2 H, 5-H, 7-H], 4.54 [t, $^3J(\text{H,H}) = 7.6 \text{ Hz}$, 2 H, NCH_2], 2.92 (s, 6 H, C1-CH₃, C3-CH₃), 2.79 (s, 3 H, C6-CH₃), 1.80 (m, 2 H, NCH_2CH_2), 1.49 (m, 2 H, CH_2CH_3), 1.00 [t, $^3J(\text{H,H}) = 7.2 \text{ Hz}$, 3 H, CH_2CH_3] ppm. $\text{C}_{16}\text{H}_{22}\text{BF}_4\text{N}$ (315.16): calcd. C 60.98, H 7.04, N 4.44; found C 70.05, H 6.88, N 4.54.

Monomethine Cyanine Dyes 3 (General Procedure): Triethylamine (0.1 mL) was added to the solution of 2-butyl-1,3-dimethyl-6-(methylthio)cyclohepta[c]pyrrolium iodide (**2**)^[13], 0.175 g, 0.5 mmol) and a corresponding quaternary salt of a nitrogen-containing heterocycle or 4-methyl-2,6-diphenylpyrylium tetrafluoroborate (0.5 mmol) in acetonitrile (3 mL). The mixture was heated at 75°C for 15 min, and was then allowed to cool to room temperature and

to stand for 4 h. The reaction was monitored by absorption spectroscopy: the disappearance of an absorption band of the methylmercapto salt (**2**) at 407 nm and increasing intensity of the desired monomethine cyanine dye band (see Table 1) were observed. The reaction mixture was concentrated under vacuum. The resulting solid was suspended in diethyl ether (10 mL). The precipitate was filtered off, washed with ethanol (1 mL) and diethyl ether ($2 \times 10 \text{ mL}$), dried and purified by recrystallization from an appropriate solvent, with addition of *N*-benzyl-*N,N*-triethylammonium tetrafluoroborate (CAS 77794–93–5, 0.5 mol) in the case of dyes **3a**, **3b** and **3d** to avoid possible precipitation of the corresponding products as mixtures of salts with different counterions. Dyes **3c** and **3e** were obtained as perchlorates after simple recrystallization, as was confirmed by elemental analysis.

Monomethine Cyanine 3a: 2-Butyl-6-[(2-butyl-1,3-dimethylcyclohepta[c]pyrrol-6(2*H*)-ylidene)methyl]-1,3-dimethylcyclohepta[c]pyrrolium tetrafluoroborate was obtained from 2-butyl-1,3-dimethyl-6-(methylthio)cyclohepta[c]pyrrolium iodide (**2**)^[13] and 2-butyl-1,3,6-trimethylcyclohepta[c]pyrrolium tetrafluoroborate (**1**). Purification was by recrystallization from ethanol with addition of *N*-benzyl-*N,N*-triethylammonium tetrafluoroborate (0.5 mmol). Yield 0.110 g (20%); m.p. 221 – 223°C . ^1H NMR: $\delta = 7.61$ [d, $^3J(\text{H,H}) = 11.2 \text{ Hz}$, 4 H, $2 \times 4\text{-H}$, 8-H], 7.04 [d, $^3J(\text{H,H}) = 11.2 \text{ Hz}$, 4 H, $2 \times 5\text{-H}$, 7-H], 6.46 (s, 1 H, C11-H), 4.09 [t, $^3J(\text{H,H}) = 8.0 \text{ Hz}$, 4 H, $2 \times \text{NCH}_2$], 2.57 (s, 12 H, $2 \times \text{C1-CH}_3$, C3-CH₃), 1.69 (m, 4 H, $2 \times \text{NCH}_2\text{CH}_2$), 1.43 (m, 4 H, $2 \times \text{CH}_2\text{CH}_3$), 0.99 [t, $^3J(\text{H,H}) = 8.8 \text{ Hz}$, 6 H, $2 \times \text{CH}_2\text{CH}_3$] ppm. $\text{C}_{31}\text{H}_{39}\text{BF}_4\text{N}_2$ (526.46): calcd. C 70.72, H 7.47, N 5.32; found C 70.48, H 7.53, N 5.45.

Monomethine Cyanine 3b: 2-Butyl-6-[(2,6-diphenyl-4*H*-pyran-4-ylidene)methyl]-1,3-dimethylcyclohepta[c]pyrrolium tetrafluoroborate was obtained from 2-butyl-1,3-dimethyl-6-(methylthio)cyclohepta[c]pyrrolium iodide (**2**) and 4-methyl-2,6-diphenylpyrylium tetrafluoroborate.^[40] Purification was by recrystallization from acetonitrile with addition of *N*-benzyl-*N,N*-triethylammonium tetrafluoroborate (0.5 mmol). Yield 0.180 g (33%); m.p. 252 – 253°C . ^1H NMR: $\delta = 8.00$ (m, 6 H, 4-H, 8-H, C₆H₅), 7.58 (m, 8 H, 5-H, 7-H, C₆H₅), 7.26 [s, 2 H, O(CCH₂)₂C], 6.79 (s, 1 H, C11-H), 3.84 [t, $^3J(\text{H,H}) = 8.0 \text{ Hz}$, 2 H, NCH_2], 2.22 (s, 6 H, C1-CH₃, C3-CH₃), 1.51 (m, 2 H, NCH_2CH_2), 1.36 (m, 2 H, CH_2CH_3), 0.98 [t, $^3J(\text{H,H}) = 8.8 \text{ Hz}$, 3 H, CH_2CH_3] ppm. $\text{C}_{33}\text{H}_{32}\text{BF}_4\text{NO}$ (545.42): calcd. C 72.67, H 5.91, N 2.57; found C 72.50, H 5.85, N 2.72.

Monomethine Cyanine 3c: 2-[(2-Butyl-1,3-dimethylcyclohepta[c]pyrrol-6(2*H*)-ylidene)methyl]-3-ethyl-1,3-benzothiazol-3-ium perchlorate was obtained from 2-butyl-1,3-dimethyl-6-(methylthio)cyclohepta[c]pyrrolium iodide (**2**) and 3-ethyl-2-methyl-1,3-benzothiazol-3-ium perchlorate.^[41] Purification was by recrystallization from ethanol. Yield 0.20 g (42%); m.p. 252 – 254°C (decomposition). ^1H NMR: $\delta = 8.19$ [d, $^3J(\text{H,H}) = 8.5 \text{ Hz}$, 1 H, BT], 8.01 [d, $^3J(\text{H,H}) = 8.4 \text{ Hz}$, 1 H, BT], 7.72 [m, 2 H, 8-H, BT], 7.58 [m, 1 H, BT], 7.49 [br. d, $^3J(\text{H,H}) = 10.5 \text{ Hz}$, 1 H, 4-H], 6.98 [br. d, $^3J(\text{H,H}) = 10.5 \text{ Hz}$, 1 H, 7-H], 6.82 [m, 2 H, 5-H C11-H], 4.65 [q, $^3J(\text{H,H}) = 7.2 \text{ Hz}$, 2 H, NCH_2CH_3], 4.08 [m, 2 H, NCH_2CH_2], 2.48 (s, 6 H, C1-CH₃, C3-CH₃), 1.63 [m, 2 H, NCH_2CH_3], 1.39 (m, 5 H, $\text{CH}_2\text{CH}_2\text{CH}_3$, NCH_2CH_3), 0.94 [t, $^3J(\text{H,H}) = 7.2 \text{ Hz}$, 3 H, $\text{CH}_2\text{CH}_2\text{CH}_3$] ppm. $\text{C}_{24}\text{H}_{27}\text{ClN}_2\text{O}_4\text{S}$ (475): calcd. C 60.69, H 5.73, N 5.90, Cl 7.46; found C 60.52, H 5.85, N 6.02, Cl 7.28.

Monomethine Cyanine 3d: 2-[(2-Butyl-1,3-dimethylcyclohepta[c]pyrrol-6(2*H*)-ylidene)methyl]-1-ethylbenzo[*c*]indolium tetrafluoroborate was obtained from 2-butyl-1,3-dimethyl-6-(methylthio)cyclohepta[c]pyrrolium iodide (**2**) and 1-ethyl-2-methylbenzo[*c*]indolium tetrafluoroborate.^[42] Purification was by recrystallization from ethanol with addition of *N*-benzyl-*N,N*-triethylammonium

tetrafluoroborate (0.5 mmol). Yield 0.180 g (36%); m.p. 118–120 °C. ^1H NMR: δ = 8.94 [d, $^3J(\text{H,H})$ = 7.6 Hz, 1 H, 3-H Bin], 8.09 [d, $^3J(\text{H,H})$ = 8.4 Hz, 1 H, 5-H Bin], 7.85 (dd, 1 H, 4-H Bin), 7.75 [d, $^3J(\text{H,H})$ = 11.0 Hz, 2 H, 4-H, 8-H], 7.67 [d, $^3J(\text{H,H})$ = 8.4 Hz, 1 H, 6-H Bin], 7.59 (m, 3 H, 5-H 7-H 7-H Bin), 7.33 [d, $^3J(\text{H,H})$ = 7.2 Hz, 1 H, 8-H Bin], 6.67 (s, 1 H, C11-H), 4.42 [q, $^3J(\text{H,H})$ = 7.6 Hz, 2 H, NCH_2CH_3], 4.10 [t, $^3J(\text{H,H})$ = 7.6 Hz, 2 H, NCH_2CH_3], 2.60 (s, 12 H, C1-CH₃ C3-CH₃), 1.73 (m, 2 H, NCH_2CH_2), 1.53 [t, $^3J(\text{H,H})$ = 6.97 Hz, 3 H, NCH_2CH_3], 1.45 (m, 2 H, CH_2CH_3), 1.01 [t, $^3J(\text{H,H})$ = 7.16 Hz, 3 H, CH_2CH_3] ppm. $\text{C}_{29}\text{H}_{31}\text{BF}_4\text{N}_2$ (494.37): calcd. C 70.45, H 6.32, N 5.67; found C 70.51, H 6.23, N 5.78.

Monomethine Cyanine 3e: 4-[(2-Butyl-1,3-dimethylcyclohepta[c]-pyrrol-6(2H)-ylidene)methyl]-1-methylquinolinium perchlorate was obtained from 2-butyl-1,3-dimethyl-6-(methylthio)cyclohepta[c]-pyrrol-6-yl iodide (**2**) and 1,4-dimethylquinolinium perchlorate.^[41] Purification was by recrystallization from ethanol. Yield 0.120 g (26%); m.p. 251–253 °C (decomposition). ^1H NMR: δ = 8.78 [d, $^3J(\text{H,H})$ = 6.4 Hz, 1 H, 2-H Q-4], 8.34 [d, $^3J(\text{H,H})$ = 8.8 Hz, 1 H, 4-H Q-4], 7.97 (m, 3 H, 3-H, 6-H, 7-H Q-4), 7.74 (m, 1 H, 5-H Q-4), 7.03 [d, $^3J(\text{H,H})$ = 11.3 Hz, 1 H, 8-H], 6.88 (m, 2 H, 3-H, 7-H), 6.65 (s, 1 H, C11-H), 6.35 [d, $^3J(\text{H,H})$ = 11.2 Hz, 1 H, 5-H], 4.39 (s, 3 H, NCH_3), 3.88 (m, 2 H, NCH_2CH_2), 2.37 (s, 6 H, C1-CH₃ C3-CH₃), 1.62 (m, 2 H, NCH_2CH_2), 1.41 (m, 2 H, CH_2CH_3), 0.99 [t, $^3J(\text{H,H})$ = 7.33 Hz, 3 H, CH_2CH_3] ppm. $\text{C}_{26}\text{H}_{29}\text{ClN}_2\text{O}_4$ (468.97): calcd. C 66.59, H 6.23, N 5.97, Cl 7.56; found C 66.36, H 6.38, N 6.05, Cl 7.42.

Monomethine Cyanine 3f: 2-[(2-Butyl-1,3-dimethylcyclohepta[c]-pyrrol-6(2H)-ylidene)methyl]-3-ethyl-1,3-benzoxazol-3-ium iodide was obtained from 2-butyl-1,3-dimethyl-6-(methylthio)cyclohepta[c]-pyrrol-6-yl iodide (**2**) and 3-ethyl-2-methyl-1,3-benzoxazol-3-ium iodide.^[41] Purification was by recrystallization from acetonitrile. Yield 0.22 g (44%); m.p. 259–260 °C. ^1H NMR: δ = 7.69 [d, $^3J(\text{H,H})$ = 8.0 Hz, 1 H, 7-H BO], 7.68 [d, $^3J(\text{H,H})$ = 11.6 Hz, 1 H, 7-H], 7.61 [d, $^3J(\text{H,H})$ = 11.6 Hz, 1 H, 8-H], 7.45 (m, 3 H, 4-H, 5-H, 6-H BO), 7.39 [d, $^3J(\text{H,H})$ = 11.6 Hz, 1 H, 4-H], 7.13 [d, $^3J(\text{H,H})$ = 11.6 Hz, 1 H, 5-H], 6.42 (s, 1 H, C11-H), 4.63 [q, $^3J(\text{H,H})$ = 7.2 Hz, 2 H, NCH_2CH_3], 4.02 (m, 2 H, NCH_2CH_2), 2.53 (s, 3 H, C1-CH₃), 2.46 (s, 3 H, C3-CH₃), 1.71 (m, 2 H, NCH_2CH_2), 1.54 [t, $^3J(\text{H,H})$ = 7.2 Hz, 3 H, NCH_2CH_3], 1.44 (m, 2 H, CH_2CH_3), 0.99 [t, $^3J(\text{H,H})$ = 7.3 Hz, 3 H, CH_2CH_3] ppm. $\text{C}_{25}\text{H}_{29}\text{IN}_2\text{O}$ (500.42): calcd. C 60.00, H 5.84, N 5.60; found C 60.12, H 5.67, N 5.82.

Acknowledgments

The authors are very grateful to Dr. Yu. L. Slominskii for helpful discussions.

- [1] A. Mishra, *Chem. Rev.* **2000**, *100*, 1973–2011.
- [2] F. Meyers, S. R. Marder, J. W. Perry, *Chem. Adv. Mater.* **1998**, *207*–269.
- [3] H. Suzuki, K. Ogura, N. Matsumoto, P. Prossposito, S. Schutzmann, *Mol. Cryst. Liq. Cryst.* **2006**, *444*, 51–59.
- [4] J. Fabian, *Chem. Rev.* **1992**, *92*, 1197–1226.
- [5] A. I. Tolmachev, Yu. L. Slominsky, A. A. Ishchemko, in: *Near-Infrared Dyes for High Technology Applications, NATO ASI Series, 3. High Technology*, vol. 52 (Eds.: S. Daehne, U. Resch-Genger, O. S. Wolfbeis), Kluwer Academic Publishers, Dordrecht, Boston, London, **1998**, pp. 385–415.
- [6] J. M. Hales, S. Zhemg, S. Barlow, S. R. Marder, J. W. Perry, *J. Am. Chem. Soc.* **2006**, *128*, 11362–11363.
- [7] W. Koenig, *J. Prakt. Chem.* **1925**, *112*, 1–36.

- [8] G. N. Lewis, M. Calvin, *Chem. Rev.* **1939**, *25*, 273–328.
- [9] G. G. Dyadyusha, A. D. Kachkovskii, *J. Inf. Recueil Mater.* **1985**, *13*, 95–104.
- [10] J. L. Bricks, N. N. Romanov, *Khim. Het. Soed. (Russ.)* **1994**, 193–194.
- [11] J. L. Bricks, E. K. Mikitenko, N. N. Romanov, *Dyes Pigm.* **1997**, *33*, 299–318.
- [12] D. G. Krotko, K. V. Fedotov, A. D. Kachkovskii, A. I. Tolmachev, *Dyes Pigm.* **2005**, *64*, 7–84.
- [13] Seitz, R. A. Olsen, T. Kämpchen, R. Matusch, *Chem. Ber.* **1979**, *112*, 2087–2094.
- [14] J. S. Craw, J. R. Reimers, G. B. Bacskey, A. T. Wong, N. S. Hush, *Chem. Phys.* **1992**, *167*, 101–109.
- [15] R. Radeaglia, *J. Prakt. Chem.* **1973**, *315*, 1121–1130.
- [16] J. Fabian, *THEOCHEM* **2006**, *766*, 49–60.
- [17] A. D. Kachkovskii, O. V. Przhonska, A. B. Ryabitzki, *THEOCHEM* **2007**, *802*, 75–83.
- [18] G. Bach, S. Daehne in *Rodd's Chemistry of Carbon Compounds* (Ed.: M. Sainsbury), Elsevier Science, Amsterdam, **1997**, vol. IVB, pp. 383–481.
- [19] H. Kuhn, *J. Chem. Phys.* **1949**, *17*, 1098–1212.
- [20] S. Webster, J. Fu, L. A. Padilha, H. Hu, O. V. Przhonska, D. J. Hagan, E. W. Van Stryland, M. V. Bondar, Yu. L. Slominsky, A. D. Kachkovskii, *J. Luminescence* **2008**, *128*, 1927–1936.
- [21] O. D. Kachkovskii, D. A. Yushchenko, G. O. Kachkovskii, N. V. Pilipchuk, *Dyes Pigm.* **2005**, *66*, 223–229.
- [22] M. J. S. Dewar, *The Molecular Orbital Theory of Organic Chemistry*, McGraw-Hill, New York, **1969**.
- [23] Z. R. Grabowski, K. Rotkiewicz, W. Rettig, *Chem. Rev.* **2003**, *103*, 3899–4031.
- [24] A. A. Ishchenko, *Usp. Khim. (Russ. Chem. Rev.)* **1991**, *60*, 865–880.
- [25] O. D. Kachkovskii, N. V. Pilipchuk, V. V. Kurdyukov, A. I. Tolmachev, *Dyes Pigm.* **2006**, *70*, 212–219.
- [26] N. Tyutyulkov, A. Gochev, F. Fratev, *Chem. Phys. Lett.* **1969**, *4*, 9–10.
- [27] J. Fabian, R. Zahradnic, *Wiss. Z. Techn. Univ. Dresden* **1997**, *26*, 315–323.
- [28] A. D. Kachkovskii, *Usp. Khim. (Russ. Chem. Rev.)* **1997**, *66*, 715–734.
- [29] A. D. Kachkovskii, *Dyes Pigm.* **1994**, *24*, 171–183.
- [30] S. Hünig, B. Ort, *Liebigs Ann. Chem.* **1984**, *12*, 1905–1935.
- [31] G. G. Dyadyusha, A. D. Kachkovskii, M. L. Dekhtyar, *Dyes Pigm.* **1991**, *16*, 173–181.
- [32] L. Brooker, *Rev. Mod. Phys.* **1942**, *14*, 275–293.
- [33] A. L. Davis, J. Keeler, E. D. Laue, D. Moskau, *J. Magn. Reson.* **1992**, *98*, 207–216.
- [34] D. J. States, R. A. Haberkorn, D. J. Ruben, *J. Magn. Reson.* **1982**, *48*, 286–292.
- [35] A. Bax, G. A. Morris, *J. Magn. Reson.* **1981**, *42*, 501–505.
- [36] M. J. Frisch, G. W. Trucks, H. B. Schlegel, G. E. Scuseria, M. A. Robb, J. R. Cheeseman, J. A. Jr Montgomery, T. Vreven, K. N. Kudin, J. C. Burant, M. Millam, S. S. Iyengar, J. Tomasi, V. Barone, B. Mennucci, M. Cossi, G. Scalmani, N. Rega, G. A. Petersson, H. Nakatsuji, M. Hada, M. Ehara, K. Toyota, R. Fukuda, J. Hasegawa, M. Ishida, T. Nakajima, Y. Honda, O. Kitao, H. Nakai, M. Klene, X. Li, J. E. Knox, H. P. Hratchian, J. B. Cross, C. Adamo, J. Jaramillo, R. Gomperts, R. E. Stratmann, O. Yazyev, A. J. Austin, R. Cammi, C. Pomelli, J. W. Ochterski, P. Y. Ayala, K. Morokuma, G. A. Voth, P. Salvador, J. J. Dannenberg, V. G. Zakrzewski, S. Dapprich, A. D. Daniels, M. C. Strain, O. Farkas, D. K. Malick, A. D. Rabuck, K. Raghavachari, J. B. Foresman, J. V. Ortiz, Q. Cui, A. G. Baboul, S. Clifford, J. Cioslowski, B. B. Stefanov, G. Liu, A. Liashenko, P. Piskorz, I. Komaromi, R. L. Martin, D. J. Fox, T. Keith, M. A. Al-Laham, C. Y. Peng, A. Nanayakkara, M. Challacombe, P. M. W. Gill, B. Johnson, W. Chen, M. W. Wong, C. Gonzalez, J. A. Pople, *GAUSSIAN03*; revision B.05, Gaussian, Inc., Pittsburgh PA, **2003**.
- [37] A. D. Becke, *J. Chem. Phys.* **1993**, *98*, 5648.

- [38] J. E. Carpenter, F. Weinhold, *THEOCHEM* **1988**, 169, 41–62.
[39] www.hyper.com.
[40] K. Dimroth, *Angew. Chem.* **1960**, 72, 331–358.
[41] A. C. Pardal, S. S. Ramos, P. F. Santos, L. V. Reis, P. Almeida, *Molecules* **2002**, 7, 320–330.
[42] N. P. Vasilenko, F. A. Mikhailenko, Yu. L. Rozhinsky, *Dyes Pigm.* **1981**, 2, 231–237.

Received: February 27, 2009
Published Online: May 27, 2009